Coastal Engineering Journal

ISSN: 2166-4250 (Print) 1793-6292 (Online) Journal homepage: www.tandfonline.com/journals/tcej20

A simple model to simulate beach state variability

Blessing Nwanosike, Dominic E. Reeve & Harshinie Karunarathna

To cite this article: Blessing Nwanosike, Dominic E. Reeve & Harshinie Karunarathna (17 Jun 2025): A simple model to simulate beach state variability, Coastal Engineering Journal, DOI: 10.1080/21664250.2025.2520084

To link to this article: https://doi.org/10.1080/21664250.2025.2520084

Published online: 17 Jun 2025.

COASTAL ENGINEERING JOURNAL
https://doi.org/10.1080/21664250.2025.2520084

A simple model to simulate beach state variability

Blessing Nwanosike, Dominic E. Reeve and Harshinie Karunarathna

Faculty of Science and Engineering, Swansea University, Swansea, UK

ABSTRACT

Predicting cross-shore profile shape is critical for understanding and managing dynamic coastal change. This study presents a novel empirical method to characterize and predict variability of cross-shore beach profile shape. The method was developed using a vast amount of synthetic cross-shore beach change data generated from the process-based coastal morphodynamic model XBeach. The model was calibrated and validated using a large-scale experimental dataset on beach profile change, ensuring accuracy and reliability of the synthetic data. The dataset replicated cross-shore beach change of a wide range of beach characteristics from a broad spectrum of wave conditions. Four cross-shore beach morphology proxies that characterise the profile shape were extracted from those data. Then, empirical relationships were derived to link them to the Dean's Number. The robustness of these relationships was tested and validated using beach profile change data from three diverse field sites and one experimental case on a gravel beach, demonstrating strong correlations and predictive capability. The findings highlight the significant role of physical drivers, such as incident wave characteristics, sediment characteristics, and beach slope, in influencing beach morphology and state transitions. This study advances the understanding of beach morphodynamics while providing a simple and practical approach for predicting profile change.

ARTICLE HISTORY
Received 6 March 2025
Accepted 10 June 2025

KEYWORDS
Dean's parameter; cross-shore beach change; XBeach; empirical beach state change model

1. Introduction and background

Coastal systems are one of the most dynamic natural systems around the world that constantly change and evolve with waves and tides (Luijendijk et al. 2018). These changes take place over a wide range of time scales, from hours to decades and longer through storms, seasonal and interannual fluctuations of wave climate, and longer-term climate change impacts (Reeve, Chadwick, and Fleming 2018; Stive 2004). This time variability is reflected in the evolution of the shoreline position for most existing proxies e.g. high water line (HWL) or mean high water (MHW) (Boak and Turner 2005) and in detailed evolution of the cross-shore beach-dune profile. In the hours to seasonal timescale, it is generally believed that beaches erode, and sediment is transported offshore during energetic/storm conditions, and they undergo natural post-storm recovery as a result of onshore sediment transport during calmer weather conditions (Angnuureng et al. 2017; Karunarathna et al. 2016; Senechal et al. 2015; Stive et al. 2002; Wright and Short 1984). Storm-driven beach erosion typically occurs over hours to days (e.g. Harley et al. 2017; Lerma et al. 2022). After a beach is rapidly eroded during a storm, the post-storm recovery is a slow process (Eichentopf et al. 2019b), typically taking weeks to months (Angnuureng et al. 2017; Castelle and Harley 2020; Phillips et al. 2019), while foredune recovery can take years to decades (Lee, Nicholls, and Birkemeier 1998; Morton, Paine, and Gibeaut 1994).

Sandy beaches in general have gentler cross-shore slopes, and sediment size decreases from the backshore to the foreshore as swash intensity decreases. When the energy dissipation is the greatest, the largest variation in sediment sizes occurs, whereas gravel beaches have a tendency for net onshore transport due to more energetic wave uprush followed by less energetic backwash (Karunarathna et al., 2012; Komar 1998; Pedrozo-Acuña et al. 2007). Smaller sediment will be eroded rapidly than larger sediment. The compound process of on-offshore sediment transport continually alters the shape of a beach profile. Provided that the beach morphology is in equilibrium with hydrodynamics, Wright and Short (1984) and Masselink and Short (1993) indicated that a cross-shore beach profile could evolve around dissipative, intermediate, and reflective states, (Figure 1), depending on the underlying hydrodynamic and sediment transport processes, which can be identified based on the values of the dimensionless fall velocity parameter (also known as the Dean's parameter, Ω), given by:

$$\Omega = H_s / w_s T_p \tag{1}$$

where H_s is the wave height in meters, T_p the peak wave period in seconds, and w_s the sediment settling velocity given in m/s.

CONTACT Harshinie Karunarathna h.u.karunarathna@swansea.ac.uk

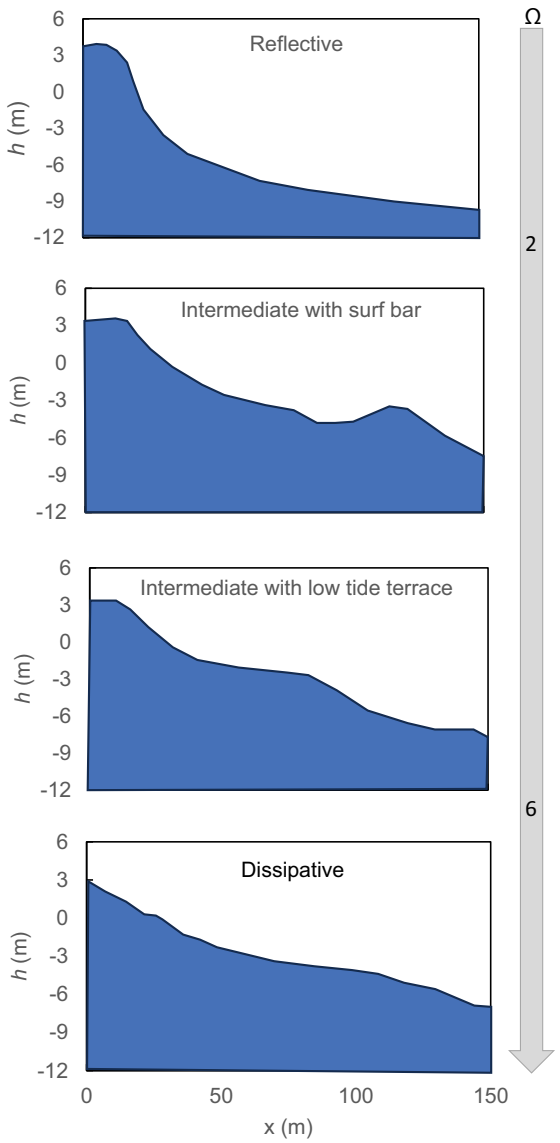

Figure 1. Simplified conceptual beach state model (after Wright and Short 1984).

Beach states can be distinguished by morphological beach features where bar and berm are two of the most striking features of the two-dimensional plane of a cross-shore beach profile (Eichentopf et al. 2019b). Beach state variability reflects either erosional or accretional sequences. An increase of Ω values indicates a shift from reflective state (steeper profiles with greater amount of sand volume) to dissipative state (gentle slopes) with a pronounced bar. On the other hand, decrease of Ω values indicates a shift from dissipative state to either intermediate or reflective state. Ranasinghe et al. (2012) and Le Cozannet et al. (2019) suggest that globally varying wave climates could be important for wave-dominated coastlines and subsequently to beach state variability.

As a state of a beach at any given time is a reflection of its incident wave energy dissipation capacity, nearshore circulation characteristics and sediment dynamics, understanding and the ability to predict beach state variability will provide significant benefits to sustainable beach management decision making. It is important to know that the beach state displayed by a given beach at a particular time largely depends on the incoming wave energy and sediment settling velocity. Sandy beaches that are exposed to large waves are typically dissipative. They are characterized by shoreward decay of incident waves over a wide surf zone. This process reverses during calmer weather when waves are smaller or less energetic and is commonly the case in the summer. This low energy beach state which is characterized by relatively steep slopes is termed "Reflective." Reflective beaches are typically steep in profile with a narrow shoaling and surf zone, composed of coarse sediment and characterized by surging breakers. When a beach morphodynamically adjusts to either more dissipative or more reflective states, it passes through a variety of intermediate states. An intermediate beach is a state between low energy reflective and high energy dissipative beach. They are commonly characterized by bar-rough topographies (Wright and Short 1984).

Several approaches can be used to predict morphological changes and beach state variability. For instance, physics-based numerical models such as XBeach (Roelvink et al. 2009; Roelvink et al. 2015), Delft3D (Lesser et al. 2004) and MIKE21 (Warren and Bach 1992) are commonly used for simulating and predicting beach morphodynamic change (e.g. Karunarathna et al. 2018; Kobayashi 2016; Kombiadou, Costas, and Roelvink 2021; Luijendijk et al., 2018; Steetzel 1993). The applications of such numerical models include simulating waves, currents, and sediment transport, illustrating changes in nearshore beach morphodynamics and hence showing beach change. These models provide a very detailed and accurate account of beach change. Numerous conceptual and empirical models have also been developed (Kriebel and Dean 1993; Larson, Erikson, and Hanson 2004; Palmsten and Holman 2012; Simmons and Splinter 2022). They are seen as a comparable alternative to highly computationally intensive numerical methods. Data-driven models which employ large scale historic datasets to forecast beach change have also been developed (e.g. Beuzen et al. 2019; Horrillo-Caraballo and Reeve 2010; Karunarathna et al. 2012; Karunarathna, Horrillo-Caraballo, and Reeve 2012; Sanuy and Jiménez 2021; Van Verseveld et al. 2015). In recent past reduced-physics and reduced-complexity modeling approaches which can be hybrids of process-based and data-driven models have been developed (Horrillo-Caraballo et al. 2014; Karunarathna, Reeve, and Spivack 2009; Reeve et al. 2019).

Utilization of numerical models, which is perhaps the most accurate method of beach change prediction, is widely known to be laborious and computationally expensive. Also, they require extensive calibration and validation before applying to a specific site, which thus demands field measurements. Data-driven models are largely site-specific and needs a large volume of historic measurements which may not be widely available. Reduced physics and empirical approaches are useful alternatives but may be limited to predictions at certain timescales or certain morphodynamic features. Also, most of them require substantial amount of historic measurements similar to data-driven approaches, which may not be widely available.

In this research, our goal is to develop a new simple and efficient empirical approach that can be used to predict beach state variability, predominantly of sandy beaches, under a wide range of wave conditions, thereby overcoming the limitations of computationally expensive process-based numerical models and the data scarcity when utilizing data-driven and other similar modeling approaches. Our method is based on generating a large quantity of synthetic beach profile change data under a wide range of wave conditions on generic sandy beaches with a wide range of characteristics. A well-calibrated and validated process-based coastal morphodynamic model is used to generate the synthetic data of cross-shore profile change of different beach types covering a range of beach slopes and sediment properties. The data is then used to develop an empirical beach state prediction model. Although a vast amount of process-based numerical simulations is initially required to develop our approach, once the method is established, it will eliminate the need to build site-specific computational models and simulate beach change from under a large number of incident wave conditions to investigate beach state change at a specific site. Instead, our method can be applied to any site to predict beach state change.

Section 2 of the paper presents the development, calibration, and validation of the numerical beach profile model used as the synthetic data generator, and the numerically simulated data. Section 3 describes the development of the empirical formulations for beach profile change and beach states. The new formulations are validated against the profile change at two field sites in Section 4. Section 5 concludes the paper.

2. Numerical model and synthetic beach profile data generation

2.1. Numerical model

The coastal morphodynamic modeling system XBeach was used to generate synthetic data of cross-shore beach profile evolution. XBeach is an open-source coastal numerical morphodynamic modeling system, which was originally developed to simulate coastal dune erosion (D. Roelvink et al. 2009). In this research, 1-D XBeach surfbeat model (XBeach-SB), which resolves waves at wave group scale, is utilized. It is assumed that waves propagate in the direction of the cross-shore profile XBeach-SB computes the propagation of short wave averaged wave envelope and accompanying longwave motion. The wave–action balance equation in the wave propagation (x) direction of (Eq. 2) is solved using a wave breaking dissipation model to derive the wave group forcing.

$$\frac{\partial A}{\partial t}+\frac{\partial c_x A}{\partial x}=-\frac{D_w+D_f}{\sigma} \tag{2}$$

where t and x are the temporal and horizontal space coordinates, respectively, A is the wave action calculated as $A=S_w(x,t)/\sigma(x,t)$. $S_w(x,t)$denotes the wave energy density, $\sigma(x,t)$ is the intrinsic wave frequency, c_x is the wave action propagation speed in the x directional space, D_w, D_f, denote the wave energy attenuation that induced by wave breaking and bottom friction respectively (Ruffini et al. 2020).

In our study, wave breaking is implemented using the Roelvink (1993) wave breaking model.

In XBeach-SB, the suspended sediment concentration in the water column is modeled using the depth-averaged advection diffusion equation with a source-sink term, based on equilibrium sediment concentrations (Galappatti and Vreugdenhil 1985), given in Eq. (3).

$$\frac{\partial hC}{\partial t}+\frac{\partial hCu^E}{\partial x}+\frac{\partial}{\partial x}\left[D_h h*\frac{\partial C}{\partial x}\right]=\frac{hC_{eq}-hC}{T_s} \tag{3}$$

In this formulation, the entrainment and deposition of sediment is determined by the difference between the equilibrium sediment concentration (C_{eq}) and the actual sediment concentration (C) which varies on the wave group time scale. The entrainment of the sediment is represented by an adaptation time (T_S) given by a simple approximation based on the local water depth (h) and sediment fall velocity (w_s). D_h is sediment diffusion coefficient, T_s is adaptation time, h is local water depth, w_s is sediment fall velocity, $u^E$is the Eulerian velocity in the x direction, and u_a is onshore directed velocity.

In the model, two sediment transport formulations available, Soulsby -Van Rijn (Soulsby 1997; Van Rijn 1984) and Van Thiel-Van Rijin (van Thiel de Vries 2009). The details of these formulations can be found in the Xbeach Manual (https://xbeach.readthedocs.io/en/latest/xbeach_manual.html). XBeach-SB allows the use of multiple sediment types, where each sediment type is determined using its own grain size.

The model simulates bed level change (z_b) using the sediment transport gradients based on Eq. (4).

$$\frac{\partial z_b}{\partial t} + \frac{f_{mor}}{(1-p)}\left(\frac{\partial q_x}{\partial x}\right) = 0 \quad (4)$$

where p is porosity, f_{mor} is a morphological acceleration factor and q_x is the sediment transport rate in the x-direction.

For further details of the XBeach-SB model, the reader is referred to the XBeach Manual (https://xbeach.readthedocs.io/en/latest/xbeach_manual.html).

2.2. Numerical model setup

The initial 1D cross-shore numerical beach profile model setup in XBeach-SB used in this study is shown in Figure 2, which has a 1:10 uniform beach slope followed by a 38 m long horizontal section, and a 3 m water depth. XBeach-SB uses a coordinate system where the computational x-axis is oriented perpendicular toward the coast and y-axis is oriented alongshore. This initial model setup replicates the laboratory experiment setup used in the RESIST (Influence of storm sequencing and beach REcovery on SedIment tranSporT and beach resilience) project funded by EU the HYDRALAB+ (https://hydralab.eu/about-hydralab/.) programme on cross-shore beach profile evolution (Eichentopf et al. 2019a). The seabed sediment has d_{50} value of 0.25 mm. The rationale for using this initial setup is to directly use the RESIST experimental data for calibration and the validation of the numerical model. The 1D numerical model was set up to replicate the laboratory wave channel, sediment characteristics, and wave conditions used in RESIST (Figure 2). A complete description of the RESIST experimental conditions can be found in Eichentopf et al. (2019a). A cross-shore varying model grid was used to improve computational efficiency, with the largest offshore grid size (Δx) of 0.75 m and the smallest nearshore grid size of 0.25 m.

Numerical simulations were first carried out under a number of different wave conditions, using the default values of the free model parameters of the XBeach model, to explore the model performance prior to calibration. p and f_{mor} of 0.3 and 1.0 were used in all simulations. When started with the plane, uniform beach profile, the profile evolution was stabilized after approximately 4 hrs. Therefore, all numerical simulations conducted in this study were of 4 hr duration.

2.3. Calibration of free model parameters and model validation

The XBeach-SB has several free calibration parameters that can be adjusted to achieve best model performance. The most common approach to model calibration is the use of manual adjustment of the key model-free parameters (Callaghan, Ranasinghe, and Roelvink 2013; Pender and Karunarathna 2013; Simmons et al. 2019; Splinter and Palmsten 2012; Stockdon et al. 2014). The sensitivity of the model outputs to the free model parameters was investigated by observing how the bed profile changed as their values were altered. Keeping all other parameters at their default values, free parameter values were changed one at a time and the model was used to simulate beach profile change from the selected wave conditions.

For modeling beach change in XBeach-SB, the influence of wave skewness (represented by the nondimensional-free parameter *facua*) on the transport of sediment appears is found to be the key mechanism which gives the greatest sensitivity (Splinter and Palmsten 2012) to model performance (Splinter and Palmsten 2012). The choice of *facua* values imposes onshore versus offshore wave-driven sediment transport. When there is a storm, it is assumed that the sediment is transported primarily offshore (*facua* = 0), and when there is calm (*facua* = 1), the sediment is transported toward the shore. To achieve the best possible balance between onshore and offshore sediment transport in the nearshore region during storm conditions, we calibrated XBeach for *facua* > 0, using the bichromatic wave conditions from the RESIST

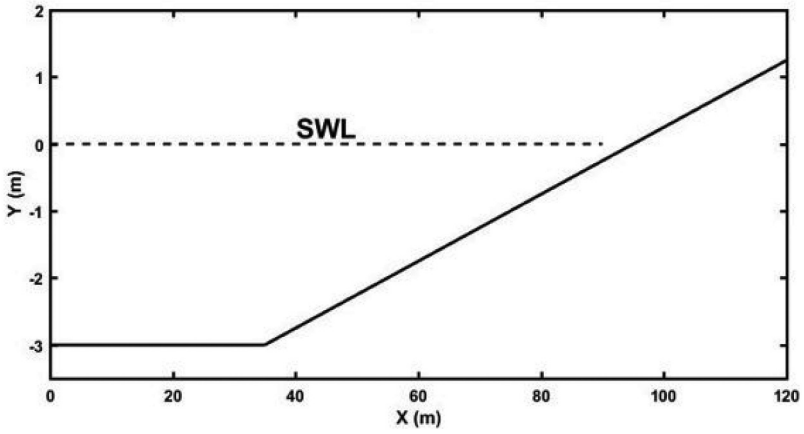

Figure 2. Numerical XBeach-SB cross-shore beach profile model set-up which replicates the RESIST experimental set-up.

experiment, given in Table 1 by comparing simulated and experimentally measured post-wave action cross-shore beach profiles.

The other two important free parameters are *eps* – threshold of drying and flooding of computational cell on the beach; and *wetslp* – critical wet slope. A sensitivity analysis involving those two parameters confirmed that the sensitivity of the model performance to them is insignificant. Therefore, the default values of *eps* = 0.005 and *wetslp* = 0.15 were used.

Figures 3 and 4 show model performance with two different *facua* values which gave the best possible outcomes for E2 (erosive) and A2 (accretive) experimental cases. Based on these results, it can be argued that the *facua* parameter should be set to 0.5 for accretive wave conditions and 0.25 for erosive wave conditions (as also suggested by Van Thiel de Vries in 2009) for storm events. It was found through an extensive calibration process that the sensitivity of the model performance is not significantly sensitive to *eps* and *wetslp*. Therefore, they were kept at the default values of *eps* = 0.005 and *wetslp* = 0.15.

The calibrated XBeach-SB model was then validated against two experimental cases, unseen during the calibration, by comparing post-wave action beach profiles simulated by the model with those measured during the RESIST experiments, given in Table 2.

Table 1. RESIST experiment bichromatic wave cases selected for model calibration.

		Component 1		Component 2	
Case	Wave type	H_1 (m)	f_1 (Hz)	H_2 (m)	f_2 (Hz)
E2 (erosive)	Bichromatic	0.245	0.3041	0.245	0.2365
A2 (accretive)	Bichromatic	0.085	0.2018	0.171	0.1755

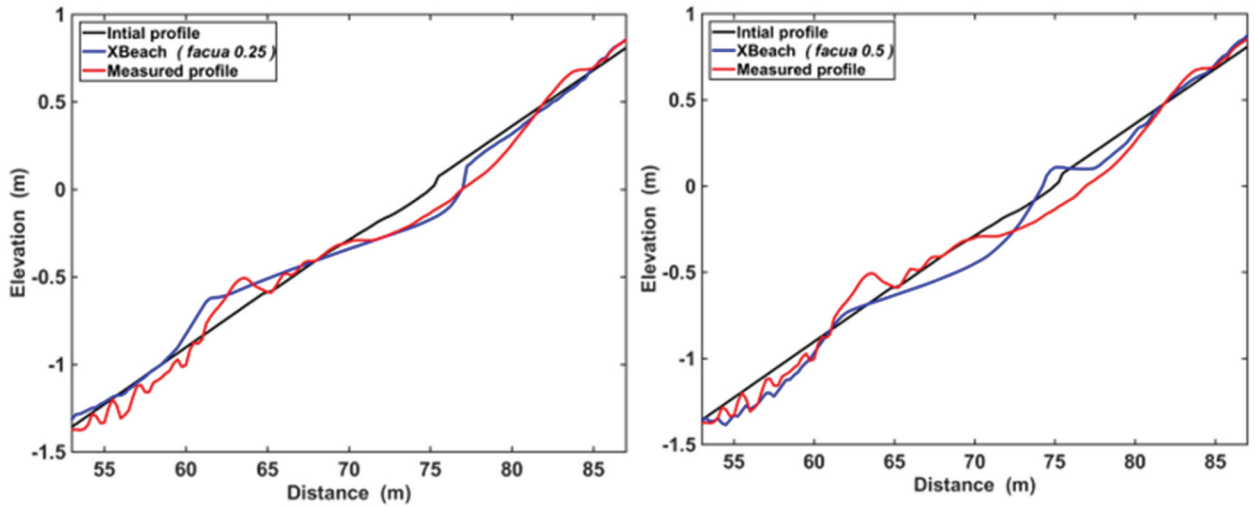

Figure 3. Post-wave action profiles with two different values for *facua* for the erosive case E2 with H_s 0.32 *m* and T_p 3.7 *s*. (left) *facua* 0.25 (right) *facua* 0.5.

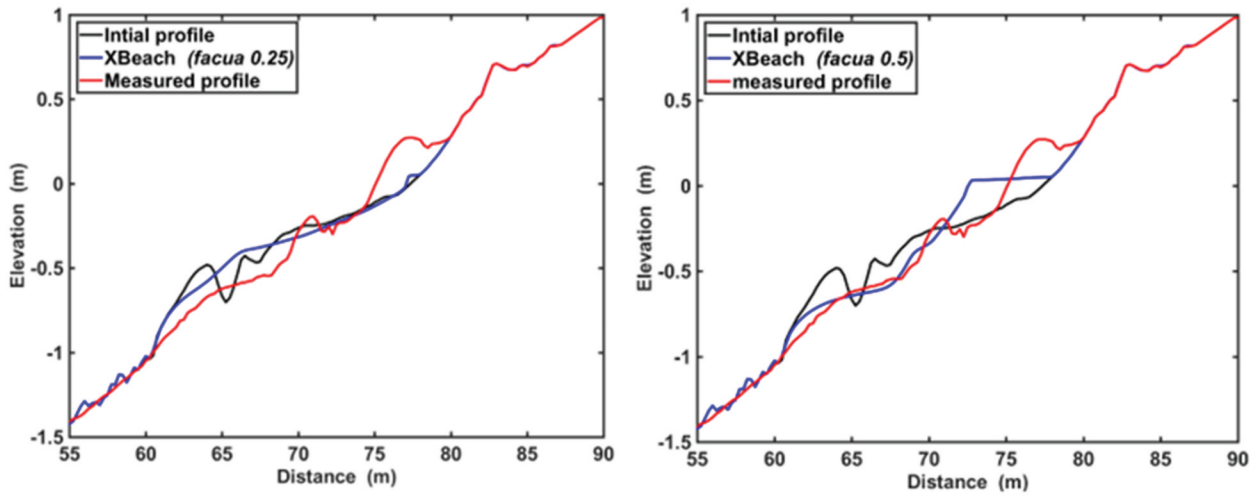

Figure 4. Post-wave action profiles with two different values for *facua* for the accretive case A2 with H_s 0.19 m and T_p 5.3 *s*. (left) *facua* 0.25 (right) *facua* 0.5.

Table 2. RESIST experiment wave cases selected for XBeach model validation.

		Component 1		Component 2	
Case	Wave type	H_1 (m)	f_1 (Hz)	H_2 (m)	f_2 (Hz)
E1 (erosive)	Bichromatic	0.320	0.3041	0.320	0.2365
A1 (accretive)	Bichromatic	0.101	0.2276	0.202	0.1976

A comparison of the modeled post-wave action beach profiles with the corresponding measured profiles for E1 and A1 is shown in Figure 5. It can be seen in those figures that the selected free model parameters captured the post-wave action erosive case well. Although the model was able to produce the berm and the bar of the accretive post-wave action profile, their location is less well captured. This is expected as XBeach-SB does not resolve individual waves.

The performance of the model was quantitatively evaluated using the Brier Skills Score (BSS) (van Rijn et al. 2003) and the Root Mean Square Error between the simulated and measured post-wave action profiles:

$$BSS = 1 - \left(\frac{\langle |x_{p-}x_m|^2 \rangle}{\langle |x_b - x_m|^2 \rangle} \right) and\ RMSE = \sqrt{\langle (Z_p - Z_m)^2 \rangle}$$

in which: x_p is the predicted profile, x_m is the measured profile, x_b is the initial profile, Z_P predicted profile, and Z_m measured profile.

Table 3 shows the classification of BSS for model performance. However, similar ranges cannot be provided for RMSE but the lower the RMSE the higher the agreement between measured and predicted profiles.

BSS values for the erosive and the accretive cases are 0.87 and 0.56, respectively. Although some specific morphodynamic features of the profile was not captured by the model, both BSS values are above the "reasonable" prediction range. RMSE values were 0.28 and 0.13 respectively, which gives confidence to use the model for simulating beach profile response from both erosive and accretive conditions modeling erosive profiles.

2.4. Numerical simulations

As seen in Section 2.2, the XBeach-SB cross-shore beach profile model satisfactorily reproduces both erosive and accretive cross-shore beach profile morphodynamic change. The model is then used to simulate profile change from wave and beach conditions covering a wide range of Ω values, representing dissipative, intermediate, and reflective beach states. The beach slopes (m) of 1:10, 1:20, 1:30, 1:50, and 1:100, and median sediment diameters (d_{50}) of 0.35, 0.43, 0.34, 0.26, and 0.18 mm were systematically and appropriately combined with random incident significant wave heights (Hs) of 0.1, 0.2, 0.3, 0.4 and 0.5 m, and peak wave period (T_p) of 1.0, 2.0, and 3.0 s to generate in total of 300 simulation scenarios. Random waves were generated using the JONSWAP wave energy spectra. The initial (pre-wave action) beach profile for all beach slopes was taken as a plane, uniform beach. Tidal water-level fluctuations were neglected at this instant.

Those simulated synthetic beach profile change will form the basis of the development of the empirical models to predict the beach state variability under different wave conditions presented in Section 3.

Table 3. Classification of brier skill score (BSS) by van Rijn et al. (2003).

Score	Classification
<0	Bad
0.0–0.3	Poor
0.3–0.6	Reasonable
0.6–0.8	Good
0.8–1.0	Excellent

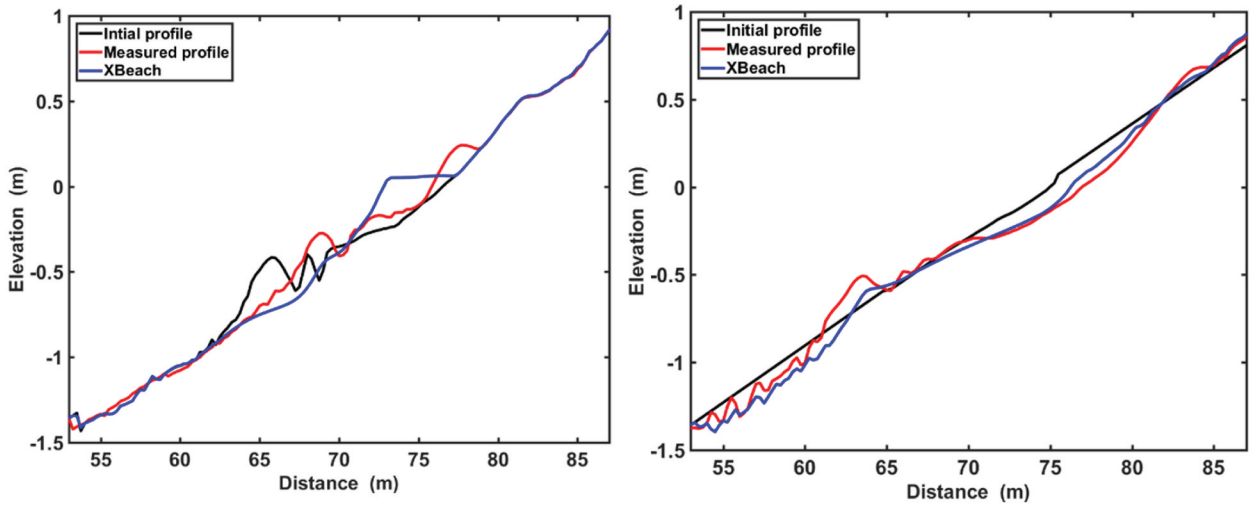

Figure 5. Comparison of the simulated profile with measured post-storm profile. Left: wave case E1 with H_s = 0.42 m and T_p = 3.7 s (erosive), and right: wave case A1 with H_s = 0.23 m and T_p = 4.7 s (accretive).

3. Development of the empirical model to predict beach state variability

The development of the empirical beach state variability formulations building on the results of different scenarios of dissipative, intermediate, and reflective beach profiles generated in Section 2 are presented here. Figure 6 gives a schematic diagram showing key beach profile features which describes the beach profile shape, considered in this development. The reference lines used were the still water level and the initial plain, uniform beach profile.

The first step in developing empirical formulation and analyzing the parameters was to generate a set of nondimensional parameters involving key profile features. In most of the engineering applications, results are presented in nondimensional form to minimize measurement errors (Kömürcü et al. 2007) and clarity. Following Buckingham's Pi theorem (Buckingham 1914; Sonin 2004), a set of nondimensional functions given in Equations (5-8) were derived for key beach profile variables shown in Figure 6 (sh_c: shoreline change at still water level; B_h: bar crest height vertically measured from the initial profile; B_c: depth of submergence of the bar crest; B_L: bar length measured with respect to the initial profile) using the variables H_s: incident significant wave height; h offshore water depth; L_0: deepwater wave length; and tan β: initial beach slope.

3.1. Beach parameter Non-dimensional quantity

Bar height

$$\left(\frac{B_h}{h}\right)^{0.5}(H_s/L_o)/Tan\beta \tag{5}$$

Bar crest

$$\left(\frac{B_c}{h}\right)^{0.5}(H_s/L_o)/Tan\beta \tag{6}$$

Bar length

$$\left(\frac{B_L}{h}\right)^{0.5}(H_s/L_o)/Tan\beta \tag{7}$$

Shoreline change

$$\left(\frac{Sh_c}{h}\right)^{0.5}(H_s/L_o)/Tan\beta \tag{8}$$

Where:

η = Derived nondimensional parameter

H_s/L_o = Wave steepness

$Tan\beta$ = initial beach slope

The nondimensional shoreline change relative to initial shoreline against Ω of all numerically simulated dissipative, intermediate, and reflective beach change scenarios are shown in Figure 7(a). It can be seen in this figure that the nondimensional shoreline change increases with increase in Ω, irrespective of the beach state. A regression analysis provides the empirical relationship between nondimensional shoreline change and Ω, given in Eq. (9) with a regression coefficient R^2 of 0.9118, which shows a strong correlation between the two quantities. Similar results for B_h, B_c, B_L are shown in Figures 7(b–d) where the relationships between their nondimensional quantities and Ω are given in Equations (10), Equation 11 and Equation 12. The R2 values of the trend lines are 0.7914, 0.9110, and 0.9528, respectively.

$$\left(\frac{Sh_c}{h}\right)^{0.5}\left(\frac{Hs}{L_0}\right)/\tan\beta = 0.1277\Omega^{1.4695} \tag{9}$$

$$\left(\frac{B_h}{h}\right)^{0.5}\left(\frac{Hs}{L_0}\right)/\tan\beta = 0.0387\Omega^{1.261} \tag{10}$$

$$\left(\frac{B_c}{h}\right)^{0.5}\left(\frac{Hs}{L_0}\right)/\tan\beta = 0.0626\Omega^{1.5214} \tag{11}$$

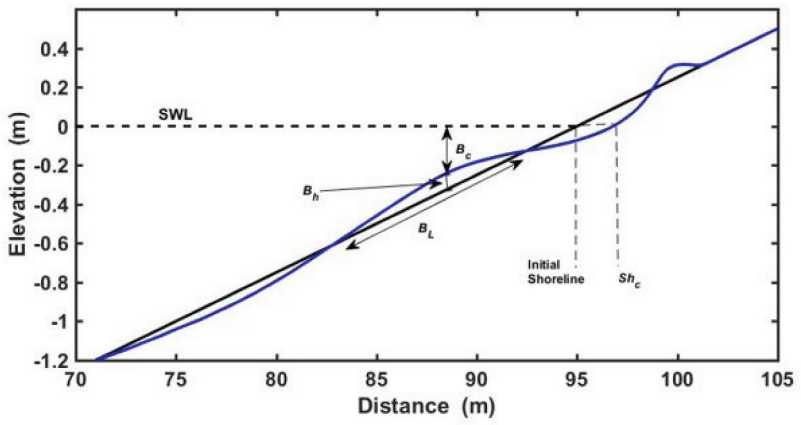

Figure 6. A schematic diagram showing key cross-shore profile parameters using in the development of the empirical model: sh_c: shoreline change at still water level; B_h: bar height vertically measured from the initial profile; B_c: depth of submergence of the bar crest; B_L: bar length measured with respect to the initial profile. Initial profile (black line), post-wave action profile (blue line).

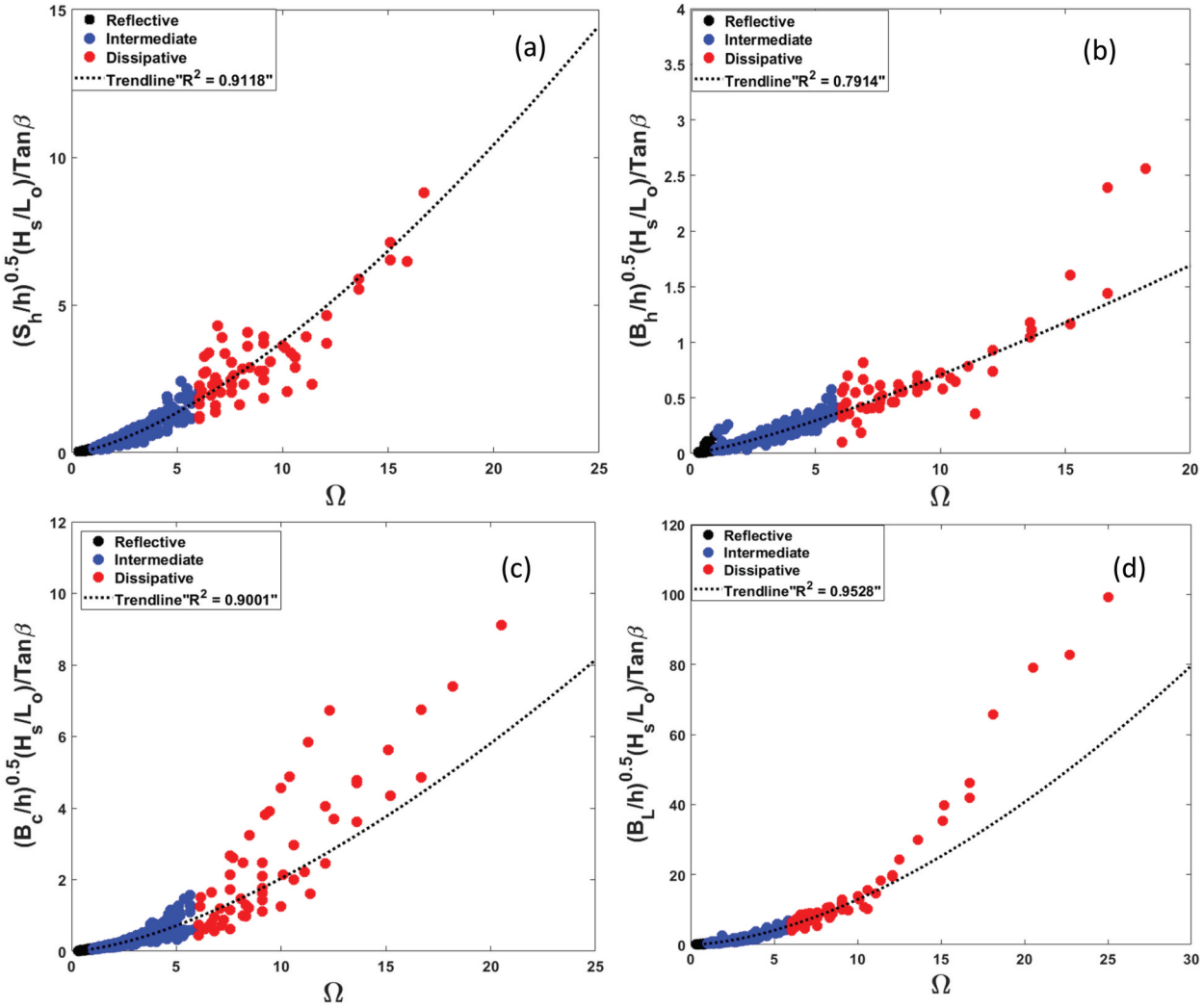

Figure 7. Non-dimensional (a) shoreline change; (b) bar crest height; (c) depth of submergence of the bar crest and (d) bar length vs. Dean's parameter Ω. Black: reflective, blue: intermediate; and red: dissipative. The best fit curve between the two quantities is shown in the dotted, broken line.

$$\left(\frac{B_c}{h}\right)^{0.5}\left(\frac{Hs}{L_0}\right)/\tan\beta = 0.2825\Omega^{1.6588} \qquad (12)$$

Equations (9)-(12) can then be used to predict the four key beach profile shape parameters and hence determine the beach profile shape under any given wave condition.

As can be seen in Figure 7, although some scatter is seen for dissipative conditions, a clear trend of variability between beach profile parameters and Ω can be seen. Scatter is expected in the dissipative cases as a result of the limitations of the XBeach-SB model in correctly simulating surf zone bar which is well documented in the literature.

4. Application of the empirical beach profile change model

In this section, the empirical formulation derived in Section 3 is applied to predict the beach profile change at three field sites with distinctly different characteristics in terms of beach slope, sediment properties, and incident wave conditions. The model performance was measured by comparing the predicted beach profile parameters with those determined from the historically measured beach profiles. The selected field sites are the Narrabeen -Collaroy beach, Australia; the Hasaki beach, Japan; and the Duck beach, North Caroline USA). The formulation was also tested against the post-wave action beach profiles measured in a laboratory on a gravel beach change by Polidoro (2018). From the available profile measurements at the four sites, a selection of cases where a distinct beach state change can be clearly seen from the pre- to post-wave action profile, is used in the preceding analysis. The wave conditions used in the model corresponding to the profile change at all field sites were the significant wave height (H_s) and the peak wave period (T_p) determined from waves measured during the period between the pre-storm profile and post-storm beach profile measurements. These two wave parameters were then given as inputs to XBeach to generate a random wave signal using the JONSWAP Spectrum, which provided the time series of wave

conditions responsible for profile change between pre- and post-wave profiles. Although using a random wave input signal derived from a single set of H_s and T_p may incur some errors if the profile change between pre- and post-wave profile occurred as a result of more than one significantly different wave conditions, this simple method is adopted to simplify the simulations and to maintain uniformity of simulations between sites.

4.1. Narrabeen-Collaroy beach, Australia

Narrabeen-Collaroy (herein referred to as Narrabeen beach) is a 3.6 km long sandy beach situated in New South Wales (NSW), Australia, located 20 km north of Sydney (Karunarathna et al. 2016). It is bounded by two headlands, Narrabeen Head in the north and Collaroy and Long Reef point in the south. Monthly surveys of five representative subaerial cross-shore beach profile lines have been done since 1976. The beach profile PF4, located at the central section of the bay, was selected for this study (Figure 8) as it is the least impacted by longshore sediment transport due to being the pivotal point of inter-annual scale beach rotation (Ranasinghe et al. 2004). Although PF4 is predominantly at intermediate state, it experiences a range of beach states depending on the antecedent wave conditions (Wright and Short 1984), tending toward more dissipative and reflective under higher and lower wave conditions (Wright, Short, and Green 1985).

Narrabeen beach is characterized by fine to medium quartz and carbonate sands with d_{50} ~0.3–0.4 mm with approximately 30% carbonate fragments shells and algae detritus. The mean spring tide range at the beach is 1.6 m (2 m maximum), and the annual average wave height of the incident waves, classified as moderate energy waves, is 1.6 m, with 20% of the waves exceeding 2 m, 5% exceeding 3 m, 1% exceeding 4 m and a very few may reach 8 m. The peak wave period is 10 s (Short and Trenaman 1992; Turner et al. 2016). Narrabeen beach's morphodynamic response is highly variable and extremely rapid due to frequent storm wave incidence. Because of the open nature of the beach, erosion, and accretion occur any time of the year (Karunarathna et al. 2014; Ranasinghe et al. 2004). In determining the beach morphodynamic variability, storm duration as well as the maximum significant wave height plays an important role (Dolan and Davis 1994; Karunarathna et al. 2014). This site was selected due to the availability of an extensive cross-shore beach profile dataset. Narrabeen beach has some of the world's best survey quality and long-time data sets from 1976 to present which incorporates both underwater hydrographic and above water beach profile surveys.

A collection of pre- and post-wave action beach profile surveys at PF4 of the Narrabeen beach shown in Figure 9 was used to validate the empirical beach profile parameter model.

4.2. Hasaki beach, Japan

The Hasaki beach is a microtidal beach located in the eastern Japan, exposed to the Pacific Ocean (Figure 10). It is a wide sandy beach characterized by longshore uniformity (Banno et al. 2020; Dastgheib et al. 2022; Kuriyama, Ito, and Yanagishima 2008). The medium grain size of the foreshore sediment is 0.18 mm (Katoh 1995). The mean high water (MHW), mean water level (MWL) and mean low water (MLW) at Hasaki beach are 1.25 m, 0.65 m, and −0.20 m, respectively, based on the datum level at Hasaki (Tokyo Peil −0.69 m) (Kuriyama 2002). The morphodynamics of Hasaki beach is dominated by a nearshore bar-trough system.

The cross-shore beach profiles measured weekly at Hasaki Oceanographic Research Station (HORS) pier are known for seasonal disparity during high energy wave conditions and calmer periods, i.e. in the autumn/winter or September to March (shoreline moves seaward) and in the spring/summer or April to August (shoreline moves landward). The sandbar moves periodically seaward during winter and landward during summer. The shoreline and the bar-trough system progradation or erosion is dependent on the season. Hasaki beach has a mean beach slope of 1/50 from −60 m to 200 m seaward and 1/20 in the deeper region (Kuriyama 2002).

The pre- and post-wave action beach profiles at the Hasaki beach, selected for empirical model validation is shown in Figure 11.

4.3. Duck beach, USA

Duck Beach is located on the east coast of the United States, in North Carolina, which has been the home of the U.S. Army Corps of Engineers Field Research Facility (Figure 12). Monthly ross-shore beach profile surveys have been collected at this site for 27 years.

The sediments at Duck beach typically include a medium-to-fine sand mixture with the grain size decreasing from 1 mm on the foreshore to 0.125 mm in the offshore zone. In the offshore region (~1 km from shore), the beach is characterized by regular shore-parallel contours, a moderate beach slope, and bars in the surf zone. An outer shore-parallel bar is present at about 4.5 m of depth, relative to the mean water level, and an inner bar is present between 1.0 and 2.0 m of depth relative to the mean water level (Horrillo-Caraballo et al. 2016).

Based on the offshore wave buoy data, it has been found that wave energy varies with season, higher during the autumn and the winter and lower during

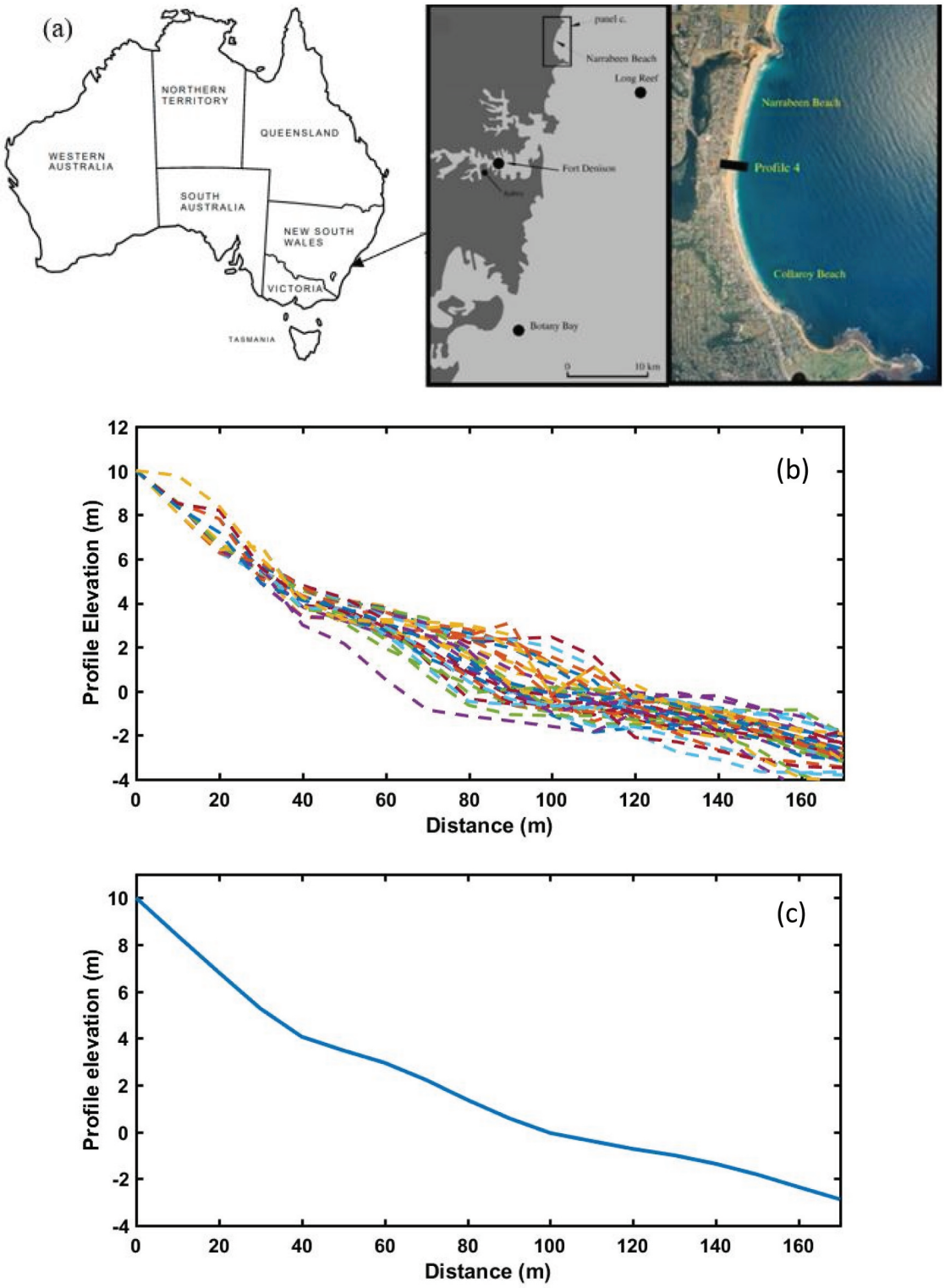

Figure 8. Narrabeen beach, New South Wales, Australia. (a) Location and view of the beach with the profile PF4 location (Karunarathna et al. 2016), (b) a selection of cross-shore survey data at profile 4 Narrabeen beach (c) mean profile determined from all beach profile surveys from 1976 to 2014.

the spring and the summer (Zhang et al. 2002). According to Horrillo-Caraballo and Reeve (2010), sand is removed from the beach face and deposited further offshore, forming sand bars during high energy wave conditions (winter) and shoreward during lower energy conditions (summer). In between high energy and milder conditions, a smoother beach profile with relatively flattened bars can also form (Holland 1998).

Pre- and post-wave action profile selected for the validation of the empirical model is given in Figure 13.

4.4. *Laboratory experiments of* Pollidoro (2018)

Although the empirical model was developed based on beach profile change in sandy beaches, it was also validated against Pollidoro (2019) laboratory

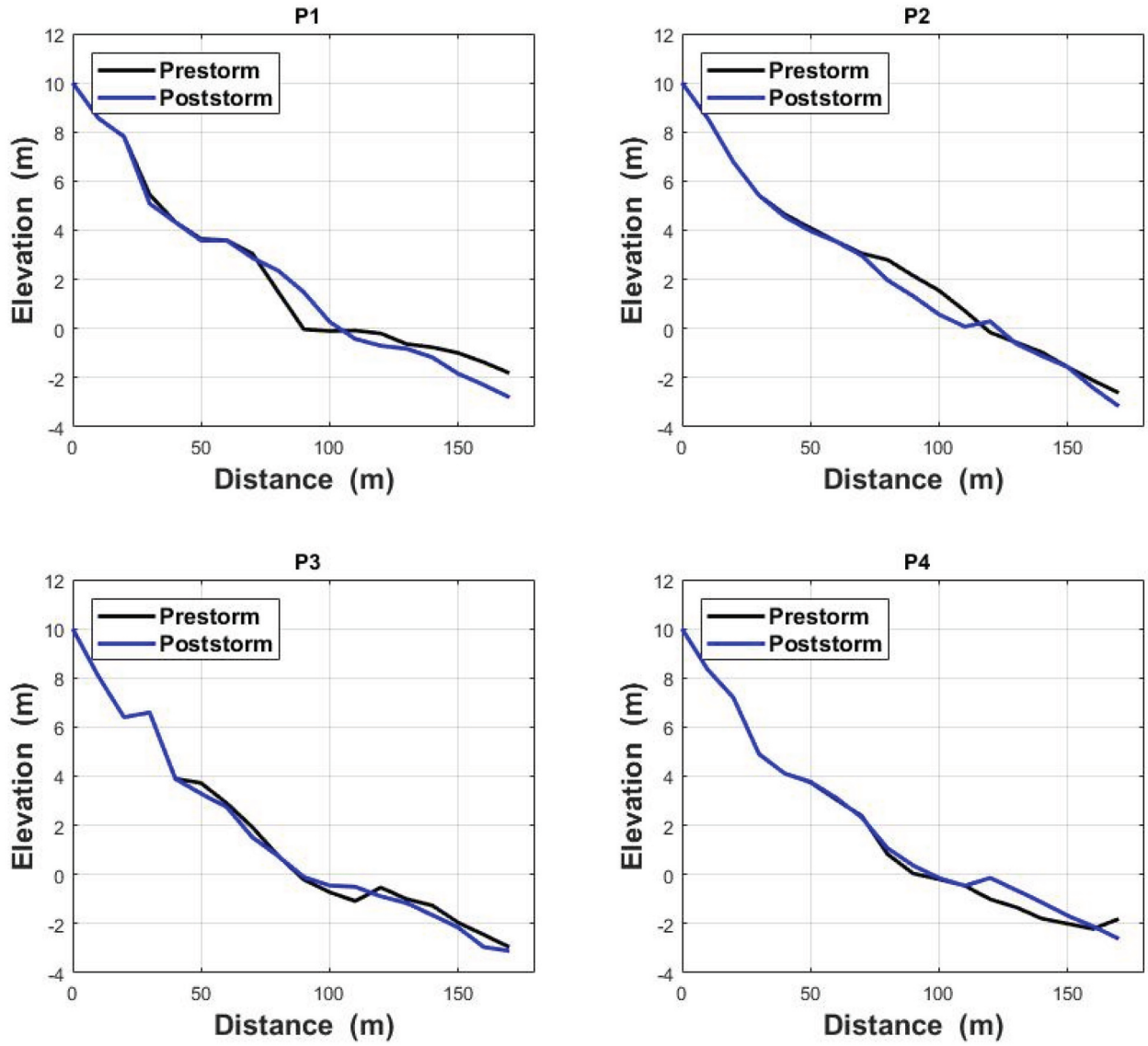

Figure 9. Some selected pre- and post-wave action profiles and wave conditions of the storm at Narrabeen beach (P1) 21/07/80–14/08/1980, *hs* 3.17m, *tp* 9.50s (P2) 27/11/1981–22/12/1981, *hs* 3.64m, *tp* 9.40s (P3) 04/08/1985–29/08/1985, *hs* 3.13m, *tp* 11.0s (P4) 05/10/1988–27/10/1988, *hs* 3.06m, *tp* 9.60s.

experiments on cross-shore profile change of a gravel beach. The experiments were conducted in a large wave flume 100 m long, 2.0 m deep, and 1.8 m wide with a 30 m long flat bathymetry, leading to a composite slope of two slopes of 1:30 (31 m long) followed by a 1:75 slope (33 m long) at HR Wallingford, UK. In this experiment, a two-dimensional (2D) physical model study was carried out to investigate the variability of a gravel beach profile under a range of wave conditions covering both uni-modal and bi-modal waves. A detailed description of this experimental study is given in Polidoro et al. (2018). The pre- and post-wave action beach profiles (under uni-modal wave action) selected for empirical model validation is shown in Figure 14.

A summary of beach characteristics of the four sites selected for model validation is given in Table 4.

Following the selection of pre- and post-wave action beach profiles, the mean beach profile at each site was determined using the entire dataset at each site. Then, the four beach parameters Sh_c, B_h, B_c and B_L were calculated from the pre- and post-wave action profiles at all cases selected at the four test cases. Then, those were non-dimensionalized using the incident wave conditions, offshore water depth, and the mean slope. Finally, the results are compared with the empirical model as shown in Figure 15 The 95% confidence intervals of the empirical formulae are shown in red dotted line.

The empirical formulations performed well at the Narrabeen beach where most cases represented intermediate beach state where most results were within the 95% confidence interval. Predictions of B_c and B_L achieved better accuracy than B_h and Sh_c. Despite

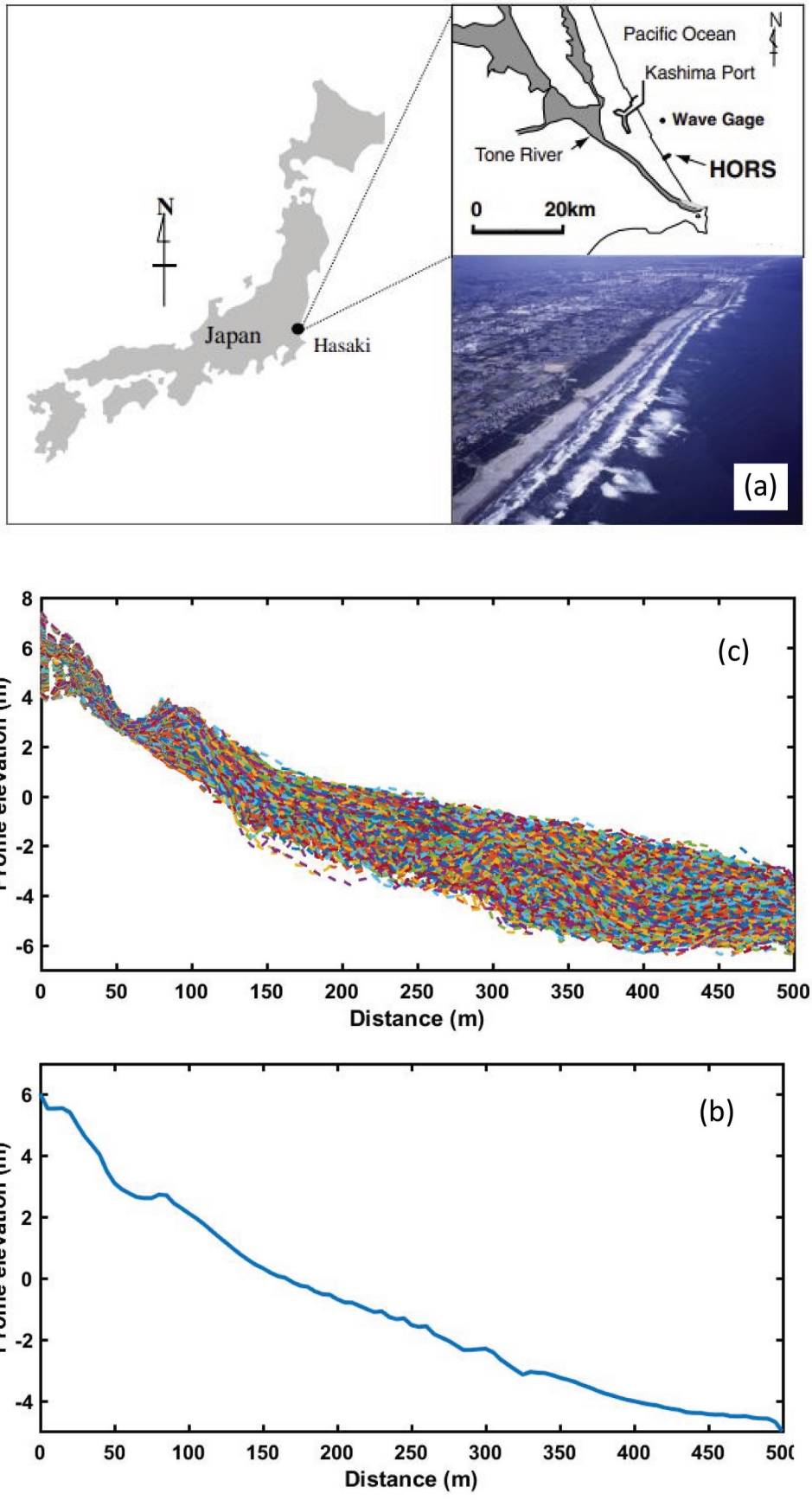

Figure 10. Hasaki beach, Japan (a) location, view of the beach and the location of HORS (Karunarathna et al. 2015), (b) cross-shore beach profiles measured at HORS during 1993–2010; and (c) mean profile determined from all measured beach profile surveys.

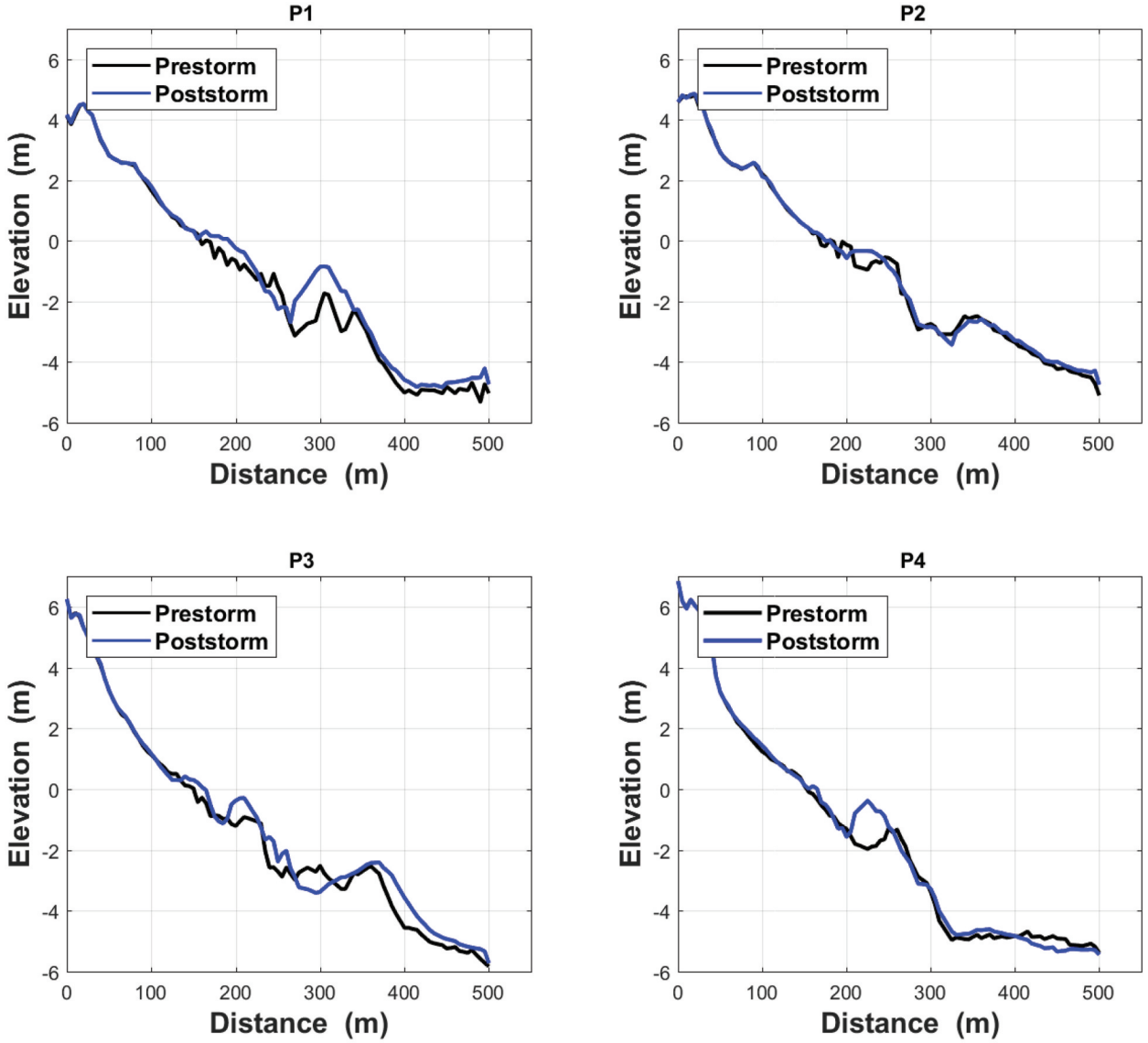

Figure 11. Some selected pre- and post-wave action profiles and wave conditions of the storm from Hasaki beach (P1) 23/01/1995–30/01/95, *hs* 2.77m, *tp* 11.9s (P2) 05/02/1996–12/02/1996, *hs* 2.77m, *ts* 11.1s (P3) 25/11/2002–2/12/2002, *Hs*3.28 m, *tp* 19.8s (P4) 16/04/2007–23/04/2007 *hs* 3.09m, *ts* 9.7s.

some deviation in shoreline change predictions, the overall results show that the empirical formulation satisfactorily capture the change in key beach profile shape parameters. The results for Polidoro (reflective) experiment also demonstrated that the empirical formulations provide highly accurate predictions. All four beach parameters were well within the 95% confidence interval of the empirical formulae. These findings underscore the robustness of the models for reflective beach states, where steep slopes and dynamic wave interactions align well with the assumptions of the empirical formulations. The empirical formulations performed less well for dissipative conditions at the Hasaki and Duck beaches. Sh_c was significantly over-predicted at both beaches. B_L at Hasaki beach is predicted well while that at Duck beach is over-predicted. B_h is mainly under-predicted at both beaches except a few cases. The prediction of B_c at Duck beach satisfactory except for two cases where the results were beyond the 95% confidence interval, while that for Hasaki beach is over-predicted except for four cases.

The differences in beach profile parameters determined from the empirical formulations and from the measured profiles can be primarily attributed to two factors: (i) the empirical model is less able to capture dissipative beach dynamics due to the limitations of the numerical model used to derive the synthetic data used to develop them; (ii) while the antecedent pre-wave action profile used in the empirical model was a uniform plane beach, the actual pre-wave action profiles at the two sites does not reflect a uniform, plane beach. Although care was taken to determine the four beach profile parameters which are derived with respect to the initial profile, some disparities

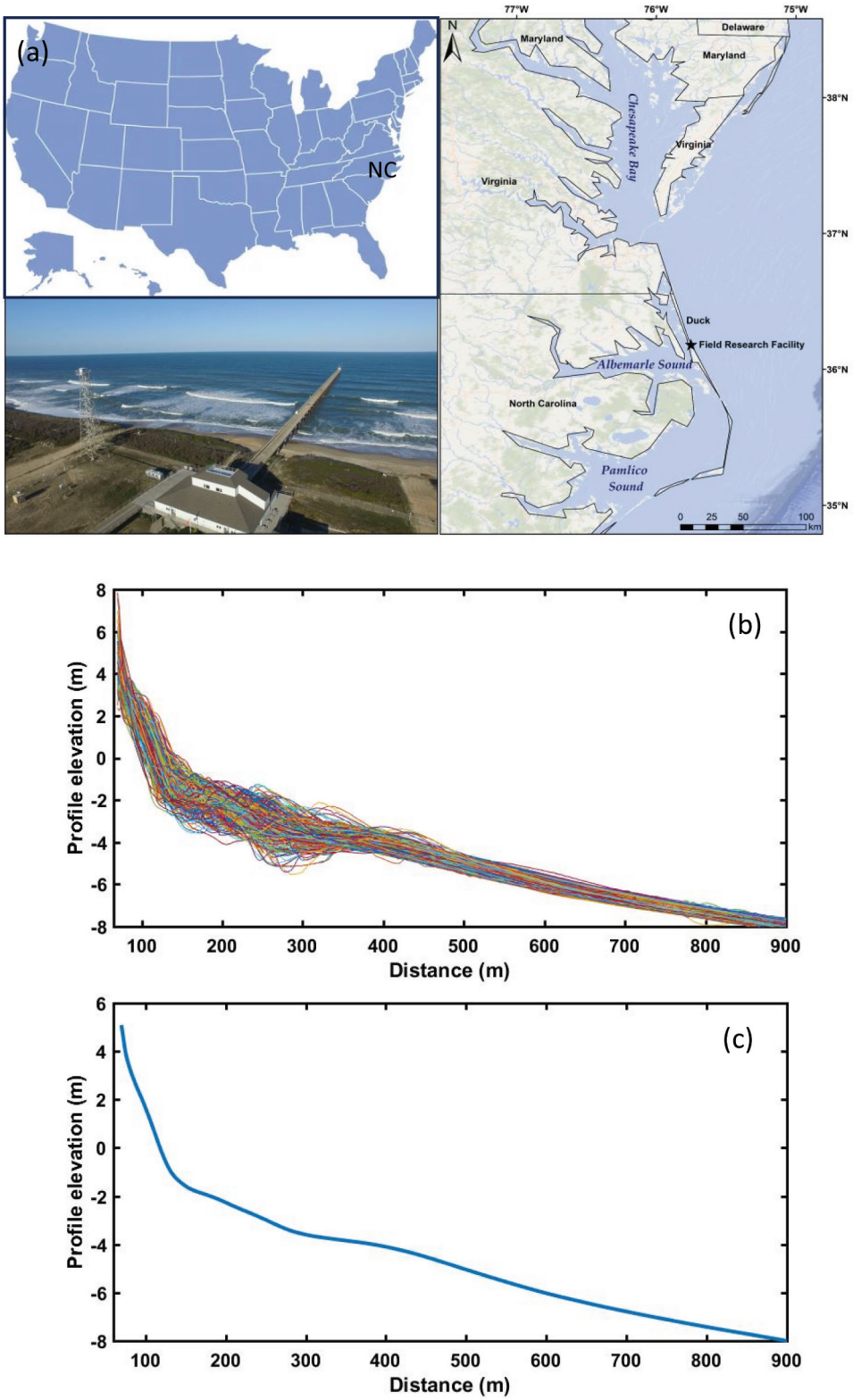

Figure 12. Duck beach, North Carolina. (a) Duck beach location and overview of the field Research Facility (FRF) pier and the observation tower (left) Holman and Mason (2020); (b) a composite plot of measured beach profile 62 at Duck; and (c) mean profile determined from all measured profile surveys.

cannot be avoided. This highlights the importance of antecedent beach profile shape in influencing beach profile morphodynamics (Masselink et al. 2023) and suggests a limitation of the formulations when applied, especially to highly dissipative beach states.

It should also be noted that the empirical model does not include the time domain but only predict the final beach state following wave action. Therefore, the dynamic beach morphodynamic change cannot be predicted.

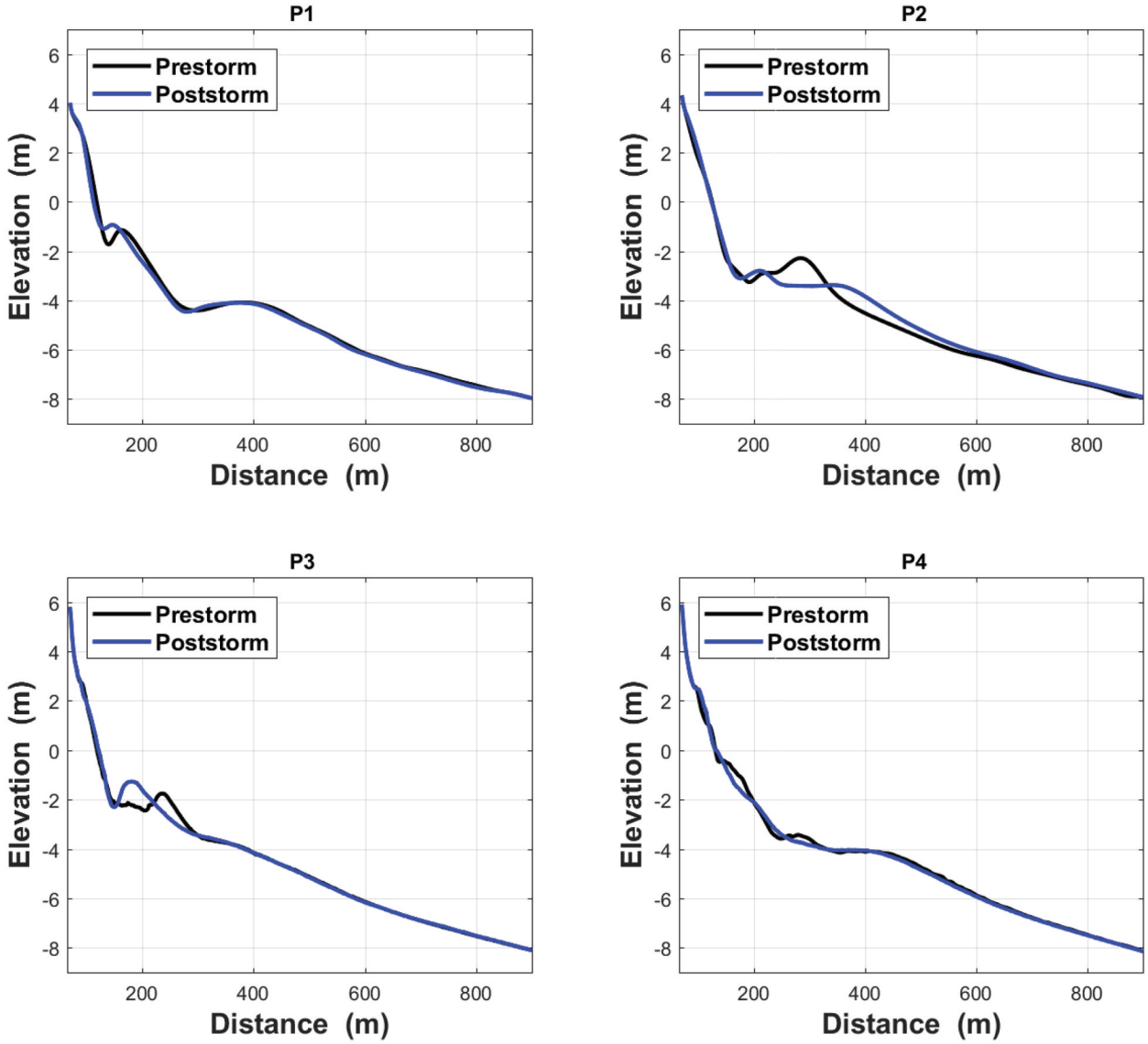

Figure 13. Some selected pre- and post-wave action profiles and wave conditions at Duck beach (P1) 31/08/1987–28/09/1987, *hs* 2.36m, *tp* 7.3s (P2) 21/02/1989–21/03/1989, *hs* 4.63m, *tp* 10.7s (P3) 23/03/1999–19/04/1999, *hs* 3.41m, *tp* 11.8s (P4) 02/05/2001–09/06/2001, *hs* 2.63m, *tp* 9.10s.

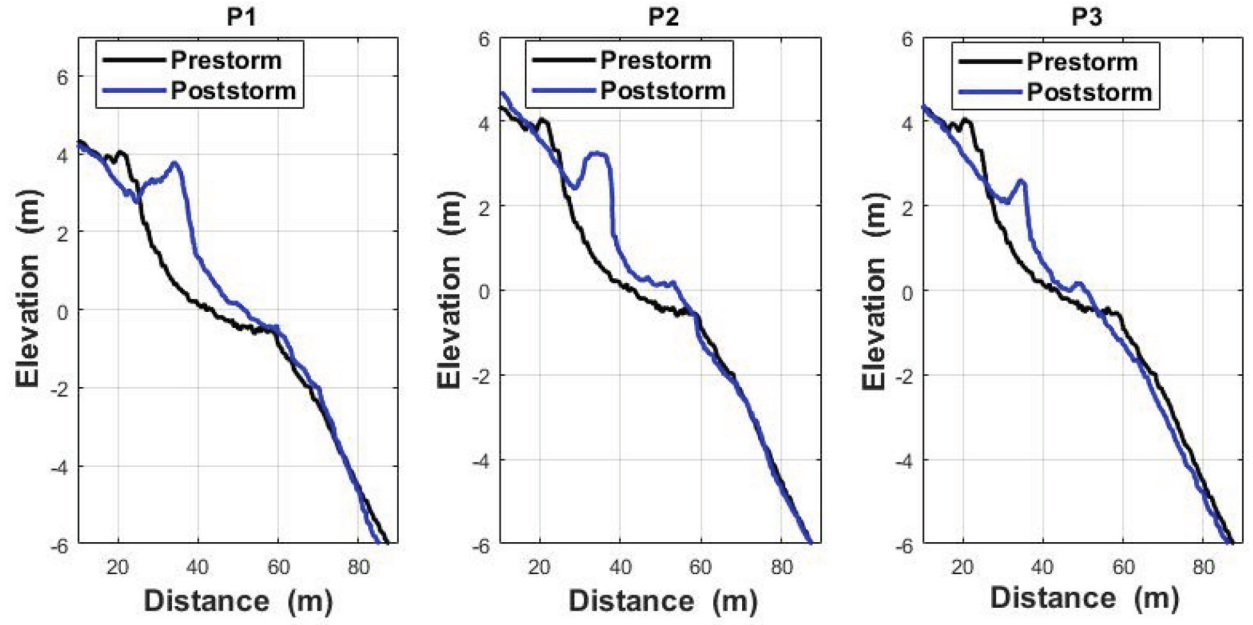

Figure 14. Some selected pre- and post-wave action beach profiles from the Polidoro et al. (2018) experiment (P1) *hs* 0.3m, *tp* 9.54s (P2) *hs* 0.3m, *tp* 8.26s (P3) *hs* 0.3m, *tp* 7.18s.

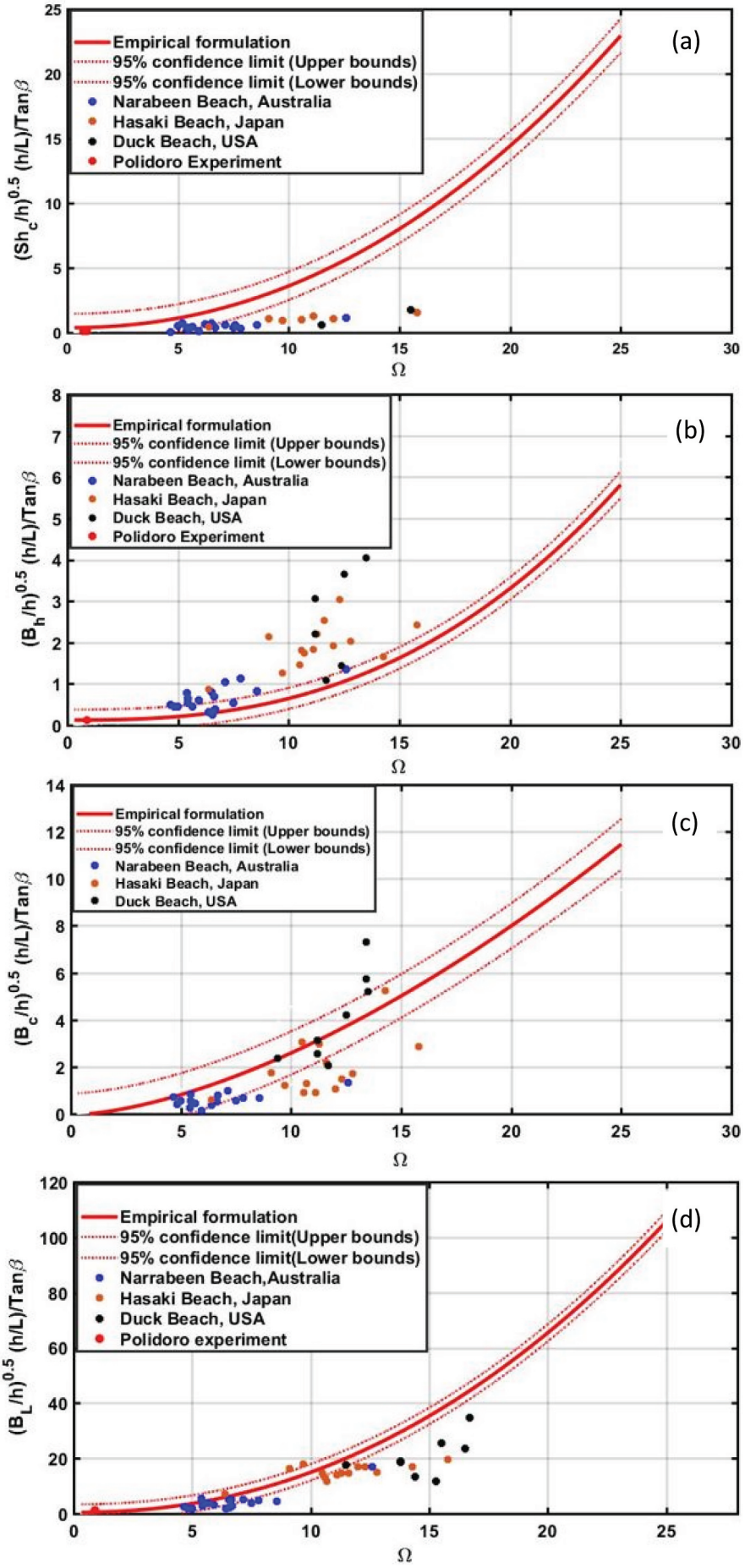

Figure 15. Comparison of (a) Sh_c, (b) B_h, (c) B_c, and (d) B_L at Narrabeen, Hasaki, and Duck beaches and Polidoro experiments with the empirical formulations. The redline is the empirical model. Red, dotted lines are the 95% confidence interval.

Table 4. Summary of beach characteristics of the four sites selected for empirical model validation.

Beach Characteristic	Narrabeen Beach	Hasaki Beach	Duke Beach, NC	Polidoro experiment
d_{50}	0.35 mm	0.2 mm	0.2 mm	15 mm
Fall velocity	0.0519(m/s)	0.0257(m/s)	0.0218(m/s)	0.4487(m/s)
Profile data period	1982 – 1992	1993 – 2010	1981 – 2006	2019
Profile type	Sandy, wave dominated, composite mean slope composite	Sandy, wave dominated, gentle mean slope	Sandy, wave dominated, composite mean slope	Gravel, steep slope
Approximate sub-tidal mean profile gradient	0.053	0.015	0.013	0.14
Wave conditions	High energy, all year-round storms	Seasonal storms	Seasonal storms	Uni- and bi-modal seas
Primary beach state	Intermediate	Dissipative	Dissipative	Reflective

5. Conclusions

This study introduced a novel empirical beach state prediction model designed to characterize and predict beach state variability driven by varying wave climates. The model provides valuable insights into how beach states evolve under different physical conditions, including wave energy, sediment properties, and beach slopes. By linking Dean's parameter (Ω) to key beach profile parameters such as shoreline change, bar height, bar crest elevation, and bar length, the study successfully advanced the understanding of beach morphodynamics.

The comparison of our empirical formulation in predicting four key parameters that define a beach profile shape clearly shows that the formulations are most effective for reflective and intermediate beaches, where they offer a reliable, cost-effective, and user-friendly tool for predicting beach profile changes. For dissipative beaches, however, the application of the formulations requires a cautious approach due to their tendency to under- or overestimate morphodynamic parameters. The implementation of these simple empirical formulations in real-world scenarios offers shoreline managers a practical approach to monitoring and addressing changes in beach conditions where expert numerical modeling skills and extensive computational resource and time requirements can be avoided.

Nonetheless, the limitations observed on predicting profile parameters in highly dissipative beaches highlight the need for further research to refine the approach, particularly through the integration of more complex pre-wave action profile characteristics and the use of a better numerical model to generate synthetic data used for the development of the approach.

Acknowledgments

The authors acknowledge the Port and Airport Research Institute of Japan (Hasaki beach data), the University of New South Wales of Australia (Narrabeen beach data), US Army Corp Field Research Facility (Duck beach data), and Dr. Andrea Polidoro (Polidoro data) for making beach profile data available for our analysis.

Author contributions

BN performed numerical simulations, developed the empirical formulations and wrote the paper. HK conceived the approach, contributed to the discussion, and revised the paper. DER supported the discussions and revising the paper.

Disclosure statement

No potential conflict of interest was reported by the author(s).

Funding

This research was funded by The Petroleum Technology Trust Fund (PTDF), Nigeria [Grants No. OSS/PHD/POF/1317/17].

ORCID

Harshinie Karunarathna http://orcid.org/0000-0002-9087-3811

References

Angnuureng, D. B., R. Almar, N. Senechal, B. Castelle, K. A. Addo, V. Marieu, and R. Ranasinghe. 2017. "Shoreline Resilience to Individual Storms and Storm Clusters on a Meso-Macrotidal Barred Beach." *Geomorphology* 290:265–276. https://doi.org/10.1016/j.geomorph.2017.04.007.

Banno, M., S. Nakamura, T. Kosako, Y. Nakagawa, S. I. Yanagishima, and Y. Kuriyama. 2020. "Long-Term Observations of Beach Variability at Hasaki, Japan." *Journal of Marine Science and Engineering* 8 (11): 871. https://doi.org/10.3390/jmse8110871.

Beuzen, T., M. D. Harley, K. D. Splinter, and I. L. Turner. 2019. "Controls of Variability in Berm and Dune Storm Erosion." *Journal of Geophysical Research: Earth Surface* 124 (11): 2647–2665. https://doi.org/10.1029/2019JF005184.

Boak, E. H., and I. L. Turner. 2005. "Shoreline Definition and Detection: A Review." *Journal of Coastal Research* 21:688–703. https://doi.org/10.2112/03-0071.1.

Buckingham, E. 1914. "On Physically Similar Systems; Illustrations of the Use of Dimensional Equations." *Physical Review* 4 (4): 345. https://doi.org/10.1103/PhysRev.4.345.

Callaghan, D. P., R. Ranasinghe, and D. Roelvink. 2013. "Probabilistic Estimation of Storm Erosion Using Analytical, Semi-Empirical, and Process Based Storm Erosion Models." *Coastal Engineering* 82:64–75. https://doi.org/10.1016/j.coastaleng.2013.08.007.

Castelle, B., and M. Harley. 2020. "Extreme Events: Impact and Recovery." *Sandy Beach Morphodynamics* 533–556.

Dastgheib, A., C. Martinez, K. Udo, and R. Ranasinghe. 2022. "Climate Change Driven Shoreline Change at Hasaki Beach Japan: A Novel Application of the Probabilistic Coastline Recession (PCR) Model." *Coastal Engineering* 172:104079. https://doi.org/10.1016/j.coastaleng.2021.104079.

Dolan, R., and R. E. Davis. 1994. "Coastal Storm Hazards." *Journal of Coastal Research* 12:103–114.

Eichentopf, S., T. Baldock, I. Caceres, D. Hurther, H. Karunarathna, M. Postacchchini, N. Ranieri, J. van der Zanden, and J. M. Alsina. 2019a. "Influence of Storm Sequencing and Beach Recovery on Sediment Transport and Beach Resilience (RESIST)." Proc. HYDRALAB+ Joint User Meeting, Bucharest, Romania.

Eichentopf, S., H. Karunarathna, and J. M. Alsina. 2019b. "Morphodynamics of Sandy Beaches Under the Influence of Storm Sequences: Current Research Status and Future Needs." *Water Science and Engineering* 12 (3): 221–234. https://doi.org/10.1016/j.wse.2019.09.007.

Galappatti, G., and C. B. Vreugdenhil. 1985. "A Depth-Integrated Model for Suspended Sediment Transport." *Journal of Hydraulic Research* 23 (4): 359–377. https://doi.org/10.1080/00221688509499345.

Harley, M. D., I. L. Turner, M. A. Kinsela, J. H. Middleton, P. J. Mumford, K. D. Splinter, M. S. Phillips, J. A. Simmons, D. J. Hanslow, and A. D. Short. 2017. "Extreme Coastal Erosion Enhanced by Anomalous Extratropical Storm Wave Direction." *Scientific Reports* 7 (1): 6033. https://doi.org/10.1038/s41598-017-05792-1.

Holland, K. T. 1998. "Beach Cusp Formation and Spacings at Duck, USA." *Continental Shelf Research* 18:1081–1098.

Holman, R. A., and C. Mason. 2020. "The Field Research Facility Research Tower." *Journal of Coastal Research* 101 (sp1): 137–140. https://doi.org/10.2112/JCR-SI101-026.1.

Horrillo-Caraballo, J. M., H. Karunarathna, S. Q. Pan, and D. Reeve. 2016. "Performance of a Data-Driven Technique Applied to Changes in Wave Height and Its Effect on Beach Response." *Water Science and Engineering* 9 (1): 42–51. https://doi.org/10.1016/j.wse.2016.02.006.

Horrillo-Caraballo, J. M., H. Karunarathna, D. E. Reeve, and S. Pan. 2014. "A Hybrid-Reduced Physics Modelling Approach Applied to the Deben Estuary, UK." International Conference in Coastal Engineering, Seoul, Korea.

Horrillo-Caraballo, J. M., and D. E. Reeve. 2010. "An Investigation of the Performance of a Data-Driven Model on Sand and Shingle Beaches." *Marine Geology* 274 (1–4): 120–134. https://doi.org/10.1016/j.margeo.2010.03.010.

Karunarathna, H., J. Brown, A. Chatzirodou, P. Dissanayake, and P. Wisse. 2018. "Multi-Timescale Morphological Modelling of a Dune-Fronted Sandy Beach." *Coastal Engineering* 136:161–171. https://doi.org/10.1016/j.coastaleng.2018.03.005.

Karunarathna, H., J. Horrillo-Caraballo, Y. Kuriyama, H. Mase, R. Ranasinghe, and D. E. Reeve. 2016. "Linkages Between Sediment composition, Wave Climate and Beach Profile Variability at Multiple Timescales." *Marine Geology* 381:194–208. https://doi.org/10.1016/j.margeo.2016.09.012.

Karunarathna, H., J. M. Horrillo-Caraballo, R. Ranasinghe, A. D. Short, and D. E. Reeve. 2012. "An Analysis of the Cross-Shore Beach Morphodynamics of a Sandy and a Composite Gravel Beach." *Marine Geology* 299:33–42. https://doi.org/10.1016/j.margeo.2011.12.011.

Karunarathna, H., J. M. Horrillo-Caraballo, R. Ranasinghe, A. D. Short, and D. E. Reeve. 2012. "An Analysis of the Cross-Shore Beach Morphodynamics of a Sandy and a Composite Gravel Beach." *Marine Geology* 299-302:33–42. https://doi.org/10.1016/j.margeo.2011.12.011.

Karunarathna, H., J. M. Horrillo-Caraballo, and D. E. Reeve. 2012. "Prediction of Cross-Shore Beach Profile Evolution Using a Diffusion Type Model." *Continental Shelf Research* 48:157–166. https://doi.org/10.1016/j.csr.2012.08.004.

Karunarathna, H., Y. Kuriyama, H. Mase, J. M. Horrillo-Caraballo, and D. E. Reeve. 2015. "Forecasts of Seasonal to Inter-Annual Beach Change Using a Reduced Physics Beach Profile Model." *Marine Geology* 365:14–20. https://doi.org/10.1016/j.margeo.2015.03.009.

Karunarathna, H., D. Pender, R. Ranasinghe, A. D. Short, and D. E. Reeve. 2014. "The Effects of Storm Clustering on Beach Profile Variability." *Marine Geology* 348:103–112. https://doi.org/10.1016/j.margeo.2013.12.007.

Karunarathna, H., D. E. Reeve, and M. Spivack. 2009. "Beach Profile Evolution as an Inverse Problem." *Continental Shelf Research* 29 (18): 2234–2239. https://doi.org/10.1016/j.csr.2009.08.016.

Katoh, K. 1995. "Changes of Sand Grain Distribution in the Surf Zone." Proceding of Coastal Dynamics' 99 Conference, New York, 335–364.

Kobayashi, N. 2016. "Coastal Sediment Transport Modeling for Engineering Applications." *Journal of Waterway, Port, Coastal, and Ocean Engineering* 142 (6): 03116001. https://doi.org/10.1061/(ASCE)WW.1943-5460.0000347.

Komar, P. D. 1998. "The 1997-98 El Niño and Erosion on the Oregon Coast." *Shore & Beach* 66 (3): 33–41.

Kombiadou, K., S. Costas, and D. Roelvink. 2021. "Simulating Destructive and Constructive Morphodynamic Processes in Steep Beaches." *Journal of Marine Science and Engineering* 9 (1): 86. https://doi.org/10.3390/jmse9010086.

Kömürcü, M.İ., İ. H. Özölçer, Ö. Yüksek, and S. Karasu. 2007. "Determination of Bar Parameters Caused by Cross-Shore Sediment Movement." *Ocean Engineering* 34 (5–6): 685–695. https://doi.org/10.1016/j.oceaneng.2006.05.005.

Kriebel, D. L., and R. G. Dean. 1993. "Convolution Method for Time-Dependent Beach-Profile Response." *Journal of Waterway, Port, Coastal, and Ocean Engineering* 119 (2): 204–226. https://doi.org/10.1061/(ASCE)0733-950X(1993)119:2(204).

Kuriyama, Y. 2002. "Medium-Term Bar Behavior and Associated Sediment Transport at Hasaki, Japan." *Journal of Geophysical Research Oceans* 107 (C9): 15–1. https://doi.org/10.1029/2001JC000899.

Kuriyama, Y., Y. Ito, and S. Yanagishima. 2008. "Medium-Term Variations of Bar Properties and Their Linkages with Environmental Factors at Hasaki, Japan." *Marine Geology* 248 (1–2): 1–10. https://doi.org/10.1016/j.margeo.2007.10.006.

Larson, M., L. Erikson, and H. Hanson. 2004. "An Analytical Model to Predict Dune Erosion Due to Wave Impact." *Coastal Engineering* 51 (8–9): 675–696. https://doi.org/10.1016/j.coastaleng.2004.07.003.

Le Cozannet, G., T. Bulteau, B. Castelle, R. Ranasinghe, G. Wöppelmann, J. Rohmer, N. Bernon, D. Idier, J. Louisor, and D. Salas-Y-Mélia. 2019. "Quantifying Uncertainties of Sandy Shoreline Change Projections as Sea Level Rises." *Scientific Reports* 9 (1): 42. https://doi.org/10.1038/s41598-018-37017-4.

Lee, G. H., R. J. Nicholls, and W. A. Birkemeier. 1998. "Storm-Driven Variability of the Beach-Nearshore Profile at Duck, North Carolina, USA, 1981–1991." *Marine Geology* 148 (3–4): 163–177. https://doi.org/10.1016/S0025-3227(98)00010-3.

Lerma, A. N., B. Castelle, V. Marieu, A. Robinet, T. Bulteau, N. Bernon, and C. Mallet. 2022. "Decadal Beach-Dune Profile Monitoring Along a 230-Km High-Energy Sandy Coast: Aquitaine, Southwest France." *Applied Geography* 139:102645. https://doi.org/10.1016/j.apgeog.2022.102645.

Lesser, G., J. A. Roelvink, J. A. T. M. Van Kester, and G. S. Stelling. 2004. "Development and Validation of a Three Dimensional Morphological Model." *Coastal Engineering* 51 (8–9): 883–915. https://doi.org/10.1016/j.coastaleng.2004.07.014.

Luijendijk, A., G. Hagenaars, R. Ranasinghe, F. Baart, G. Donchyts, and S. Aarninkhof. 2018. "The State of the world's Beaches." *Scientific Reports* 8 (1): 6641. https://doi.org/10.1038/s41598-018-24630-6.

Masselink, G., B. Castelle, T. Scott, and A. Kosnstantinou. 2023. "Role of Atmospheric Indices in Describing Shoreline Variability Along the Atlantic Coast of Europ." *Geophysical Research Letter* 50 (22). https://doi.org/10.1029/2023GL106019.

Masselink, G., and A. D. Short. 1993. "The Effect of Tide Range on Beach Morphodynamics and Morphology: A Conceptual Beach Model." *Journal of Coastal Research* 9 (3): 785–800.

Morton, R. A., J. G. Paine, and J. C. Gibeaut. 1994. "Stages and Durations of Post-Storm Beach Recovery, Southeastern Texas Coast, USA." *Journal of Coastal Research* 10 (4): 884–908. https://www.jstor.org/stable/4298283.

Palmsten, M. L., and R. A. Holman. 2012. "Laboratory investigation of dune erosion using stereo video." *Coastal Engineering* 60:123–135. https://doi.org/10.1016/j.coastaleng.2011.09.003.

Pedrozo-Acuña, A., D. J. Simmonds, A. J. Chadwick, and R. Silva. 2007. "A Numerical–Empirical Approach for Evaluating Morphodynamic Processes on Gravel and Mixed Sand–Gravel Beaches." *Marine Geology* 241 (1–4): 1–18. https://doi.org/10.1016/j.margeo.2007.02.013.

Pender, D., and H. Karunarathna. 2013. "A Statistical Process Based Approach for Modelling Beach Profile Variability." *Coastal Engineering* 81:19–29. https://doi.org/10.1016/j.coastaleng.2013.06.006.

Phillips, M. S., C. E. Blenkinsopp, K. D. Splinter, M. D. Harley, and I. L. Turner. 2019. "Modes of Berm and Beach Face Recovery Following Storm Reset: Observations Using a Continuously Scanning Lidar." *Journal of Geophysical Research: Earth Surface* 124 (3): 720–736. https://doi.org/10.1029/2018JF004895.

Polidoro, A. 2019. "The Effect of Grain Size Distribution and Bimodal Sea States on Coarse Beach Sediment Dynamics." PhD Thesis, The Open University.

Polidoro, A., T. Pullen, J. Eade, T. Mason, B. Blanco, and D. Wyncoll. 2018. "Gravel Beach Profile Response Allowing for Bimodal Sea States." *Maritime Engineering* 171:145–166.

Ranasinghe, R., R. Holman, M. de Schipper, T. Lippmann, J. Wehof, T. M. Duong, D. Roelvink, and M. Stive. 2012. "Quantifying Nearshore Morphological Recovery Time Scales Using Argus Video Imaging: Palm Beach, Sydney and Duck, North Carolina." *Coastal Engineering Proceedings* 1 (33): 24. https://doi.org/10.9753/icce.v33.sediment.24.

Ranasinghe, R., R. McLoughlin, A. Short, and G. Symonds. 2004. "The Southern Oscillation Index, Wave Climate, and Beach Rotation." *Marine Geology* 204 (3–4): 273–287. https://doi.org/10.1016/S0025-3227(04)00002-7.

Reeve, D., A. Chadwick, and C. Fleming. 2018. *Coastal Engineering: Processes, Theory and Design Practice*. Taulor and Francis Group, CRC Press.

Reeve, D. E., J. Horrillo-Caraballo, H. Karunarathna, and S. Pan. 2019. "A New Perspective on Meso-Scale Shoreline Dynamics Through Data-Driven Analysis." *Geomorphology* 341:169–191. https://doi.org/10.1016/j.geomorph.2019.04.033.

Roelvink, D., A. Reniers, A. P. Van Dongeren, J. V. T. De Vries, R. McCall, and J. Lescinski. 2009. "Modelling Storm Impacts on Beaches, Dunes and Barrier Islands." *Coastal Engineering* 56 (11–12): 1133–1152. https://doi.org/10.1016/j.coastaleng.2009.08.006.

Roelvink, J. A. 1993. "Dissipation in Random Wave Groups Incident on a Beach." *Coastal Engineering* 19 (1–2): 127–150. https://doi.org/10.1016/0378-3839(93)90021-Y.

Roelvink, V. D., A. P. Van Dongeren, R. McCall, B. Hoonhout, A. van Rooijen, P. van Geer, L. De Vet, K. Nederhoff, and E. Quataert. 2015. "XBeach Technical Reference: Kingsday Release. Model Description and Reference Guide to Functionalities."

Ruffini, G., R. Briganti, J. M. Alsina, M. Brocchini, N. Dodd, and R. McCall. 2020. "Numerical Modeling of Flow and Bed Evolution of Bichromatic Wave Groups on an Intermediate Beach Using Nonhydrostatic XBeach." *Journal of Waterway, Port, Coastal, and Ocean Engineering* 146 (1): 04019034. https://doi.org/10.1061/(ASCE)WW.1943-5460.0000530.

Sanuy, M., and J. A. Jiménez. 2021. "Probabilistic Characterisation of Coastal Storm-Induced Risks Using Bayesian Networks." *Natural Hazards and Earth System Sciences Discussions* 21:219–238. https://doi.org/10.5194/nhess-21-219-2021.

Senechal, N., G. Coco, B. Castelle, and V. Marieu. 2015. "Storm Impact on the Seasonal Shoreline Dynamics of a Meso-To Macrotidal Open Sandy Beach (biscarrosse, France)." *Geomorphology* 228:448–461. https://doi.org/10.1016/j.geomorph.2014.09.025.

Short, A. D., and N. L. Trenaman. 1992. "Wave Climate of the Sydney region, an Energetic and Highly Variable Ocean Wave Regime." *Marine and Freshwater Research* 43 (4): 765–791. https://doi.org/10.1071/MF9920765.

Simmons, J. A., and K. D. Splinter. 2022. "A Multi-Model Ensemble Approach to Coastal Storm Erosion Prediction." *Environmental Modelling & Software* 150:105356. https://doi.org/10.1016/j.envsoft.2022.105356.

Simmons, J. A., K. D. Splinter, M. D. Harley, and I. L. Turner. 2019. "Calibration Data Requirements for Modelling Subaerial Beach Storm Erosion." *Coastal Engineering* 152:103507. https://doi.org/10.1016/j.coastaleng.2019.103507.

Sonin, A. A. 2004. "A Generalization of the Π-Theorem and Dimensional Analysis." *Proceedings of the National Academy of Sciences* 101 (23): 8525–8526. https://doi.org/10.1073/pnas.0402931101.

Soulsby, R. L. 1997. *Dynamics of Marine Sands*. 1st ed. London: Thomas Telford.

Splinter, K. D., and M. L. Palmsten. 2012. "Modeling Dune Response to an East Coast Low." *Marine Geology* 329:46–57. https://doi.org/10.1016/j.margeo.2012.09.005.

Steetzel, H. J. 1993. "Cross-Shore Transport During Storm Surges." PhD Thesis, Technical University of Delft.

Stive, M. J. 2004. "How Important is Global Warming for Coastal Erosion?" *Climatic Change* 64 (1/2): 27. https://doi.org/10.1023/B:CLIM.0000024785.91858.1d.

Stive, M. J., S. G. Aarninkhof, L. Hamm, H. Hanson, M. Larson, K. M. Wijnberg, R. J. Nicholls, and M. Capobianco. 2002. "Variability of Shore and Shoreline Evolution." *Coastal Engineering* 47 (2): 211–235. https://doi.org/10.1016/S0378-3839(02)00126-6.

Stockdon, H. F., D. M. Thompson, N. G. Plant, and J. W. Long. 2014. "Evaluation of Wave Runup Predictions from Numerical and Parametric Models." *Coastal Engineering* 92:1–11. https://doi.org/10.1016/j.coastaleng.2014.06.004.

Turner, I. L., M. D. Harley, A. D. Short, J. A. Simmons, M. A. Bracs, M. S. Phillips, and K. D. Splinter. 2016. "A Multi-Decade Dataset of Monthly Beach Profile Surveys and Inshore Wave Forcing at Narrabeen, Australia." *Scientific Data* 3 (1): 1–13. https://doi.org/10.1038/sdata.2016.24.

Van Rijn, L. C. 1984. "Sediment Transport, Part III: Bed Forms and Alluvial Roughness." *Journal of Hydraulic Engineering* 110 (12): 1733–1754. https://doi.org/10.1061/(ASCE)0733-9429(1984)110:12(1733).

van Rijn, L. C., D. J. Walstra, B. Grasmeijer, J. Sutherland, S. Pan, and J. P. Sierra. 2003. "The Predictability of Cross-Shore Bed Evolution of Sandy Beaches at the Time Scale of Storms and Seasons Using Process-Based Profile Models." *Coastal Engineering* 47 (3): 295–327. https://doi.org/10.1016/S0378-3839(02)00120-5.

van Thiel de Vries, J. S. M. 2009. "Dune Erosion During Storm Surges."

Van Verseveld, H. C. W., A. R. Van Dongeren, N. G. Plant, W. S. Jäger, and C. Den Heijer. 2015. "Modelling Multi-Hazard Hurricane Damages on an Urbanized Coast with a Bayesian Network Approach." *Coastal Engineering* 103:1–14. https://doi.org/10.1016/j.coastaleng.2015.05.006.

Warren, I. R., and H. Bach. 1992. "MIKE 21: A Modelling System for Estuaries, Coastal Waters and Seas." *Environmental Software* 7 (4): 7229–7240. https://doi.org/10.1016/0266-9838(92)90006-P.

Wright, L. D., and A. D. Short. 1984. "Morphodynamic Variability of Surf Zones and Beaches: A Synthesis." *Marine Geology* 56 (1–4): 93–118. https://doi.org/10.1016/0025-3227(84)90008-2.

Wright, L. D., A. D. Short, and M. O. Green. 1985. "Short-Term Changes in the Morphodynamic States of Beaches and Surf Zones: An Empirical Predictive Model." *Marine Geology* 62 (3–4): 339–364. https://doi.org/10.1016/0025-3227(85)90123-9.

XBeach Manual. "XBeach User Manual." Accessed October. 2020. https://xbeach.readthedocs.io/en/latest/xbeach_manual.html.

Zhang, K., W. Huang, B. C. Douglas, and S. Leatherman. 2002. "Shoreline Position Variability and Long-Term Trend Analysis." *Shore & Beach* 70 (2): 31–35.